

## PERSPECTIVE

[View Article Online](#)  
[View Journal](#) | [View Issue](#)Cite this: *Dalton Trans.*, 2020, **49**,  
1351Received 16th November 2019,  
Accepted 17th December 2019

DOI: 10.1039/c9dt04763h

[rsc.li/dalton](http://rsc.li/dalton)The unique  $\beta$ -diketiminate ligand in aluminum(i) and gallium(i) chemistryMingdong Zhong,<sup>id</sup> Soumen Sinhababu<sup>id</sup> and Herbert W. Roesky<sup>id</sup>\*

Over the past few decades,  $\beta$ -diketiminate ligands have been widely used in coordination chemistry and are capable of stabilizing various metal complexes in multiple oxidation states. Recently, the chemistry of aluminum and gallium in their +1 oxidation state has rapidly emerged.  $\text{NacNacM(i)}$  ( $\text{M} = \text{Al, Ga}$ ;  $\text{NacNac} = \beta$ -diketiminate ligand) shows a two coordinate metal center comparable with singlet carbene-like species. The metal center also possesses a formally vacant p-orbital. In this article we present an overview of the last 10 years for aluminum(i) and gallium(i) stabilized by  $\beta$ -diketiminate ligands that have been widely explored in bond breaking and forming species.

## 1. Introduction

Complexes containing a low-oxidation metal center is a key topic in modern organometallic chemistry as it leads to the development of new systems. A number of transition metal complexes were synthesized in a broad range of oxidation states to activate small molecules or used as catalysts in organic reactions.<sup>1</sup> It was not until 1991 that the first structurally characterized molecular aluminum(i) compound was reported.<sup>2</sup> Since then, the chemistry of Group 13 metals in the +1 oxidation state have played a great part in the development of p-block chemistry. The synthesis of compounds with aluminum and gallium in the +1 oxidation state is experimentally challenging and consistently hampered by their high reactivity and pronounced tendency towards disproportionation.<sup>3</sup> The lone pair of electrons in  $\text{MR}$  ( $\text{R} = \beta$ -diketiminate) ( $\text{M} = \text{Al, Ga}$ ) compounds can act as a basic site towards a range of Lewis acids, forming a  $\sigma$  donating bond.<sup>4</sup> Donor-acceptor bonds have been observed in a range of main group elements, transition metals, and lanthanide and actinide metal complexes. The general  $\text{M}^{\text{I}}\text{R}$  unit ( $\text{M} = \text{Al, Ga}$ ) can be considered isolobal with singlet carbenes, CO, and CNR.

$\beta$ -Diketiminates have found widespread application as supporting ligands in metal-mediated catalysis.<sup>5</sup> The stoichiometric transformations of  $\text{NacNacAl(i)}$  and  $\text{NacNacGa(i)}$  have also been explored widely owing to the lone pair of electrons and a formally vacant p-orbital on aluminum affording high electrophilic and nucleophilic reactivity.<sup>6</sup> A comparison between main group elements and transition metals was drawn when main group species were found to have reactivity

towards small molecules under ambient conditions. This was rationalized by main group species possessing donor/acceptor frontier orbitals which are separated by modest energy gaps, thus drawing comparisons with open-shell transition metal species.<sup>7</sup> In 2000, Roesky *et al.* chose the  $\beta$ -diketiminate ligand to synthesize a more kinetically stable monomeric aluminum(i) compound  $\text{Al}\{\text{HC}[\text{C}(\text{Me})\text{NDipp}]_2\}$  ( $\text{Dipp} = 2,6\text{-}^i\text{Pr}_2\text{C}_6\text{H}_3$ ) (**1**).<sup>8a</sup> This was the first stable dicoordinate aluminum(i) compound to be prepared and structurally characterized in the solid-state. Later, Cui *et al.* also reported a  $\beta$ -diketiminate ligand stabilized aluminum(i) compound  $\text{Al}\{\text{HC}[\text{C}(\text{Bu})\text{NDipp}]_2\}$ .<sup>8b</sup> Computational studies of  $\beta$ -diketiminate stabilized heavier group metal complexes have shown that their metal lone pairs are associated with the HOMO-2.<sup>9</sup> As a result, they are good  $\sigma$  donor ligands and poor  $\pi$  acceptors like N-heterocyclic carbenes (NHCs), and thus have the potential to display carbene-like chemistry. Inoue *et al.* reported the first neutral  $\text{Al(i)}$  compound containing an  $\text{Al}=\text{Al}$  double bond, which was achieved through the reductive dimerization of the corresponding N-heterocyclic carbene (NHC)-stabilized silyl substituted aluminum(iii) dihalide (**I**, Fig. 1), and its reactivity toward the fixation and selective reduction of  $\text{CO}_2$ , both of which can be accessed in a stoichiometric and catalytic fashion.<sup>10</sup> In 2018, Aldridge and Goicoechea *et al.* reported the first isolation of a nucleophilic aluminyl anion  $[(\text{NON})\text{Al}]^-$  by employing a chelating ligand ( $\text{NON} = 4,5\text{-bis}(2,6\text{-diisopropylanilido})\text{-}2,7\text{-di-tert-butyl-}9,9\text{-dimethylxanthene}$ ) (**II**, Fig. 1), which acts as an unprecedented aluminum(i) nucleophile (*e.g.*, in reactions with  $^t\text{Bu}_3\text{PAuI}$ ), and which effects the formal oxidative addition of the C-C bond in benzene.<sup>11</sup> After that, Coles and co-workers also synthesized a two-coordinate N-heterocyclic aluminyl anion  $\text{K}[\text{Al}(\text{NON}^{\text{Dipp}})]$  ( $\text{NON}^{\text{Dipp}} = [\text{O}(\text{SiMe}_2\text{NDipp})_2]^{2-}$ ,  $\text{Dipp} = 2,6\text{-}^i\text{Pr}_2\text{C}_6\text{H}_3$ , **III**, Fig. 1), which is able to undergo further reactions such as activation of elemental selenium to form an

Universität Göttingen, Institut für Anorganische Chemie, Tammannstrasse 4,  
D-37077 Göttingen, Germany. E-mail: [hroesky@gwdg.de](mailto:hroesky@gwdg.de)



**Fig. 1** Di-*tert*-butyl(methyl)silyl-substituted dialumene (II), anionic group 13 analogues of *N*-heterocyclic carbenes (II–III), monomeric 1,2,4-tri-*tert*-butylcyclopentadienylaluminum(I) (IV), Lewis base stabilized aluminum(I) hydride (V) and an alkyl-substituted aluminum anion (VI).

aluminum complex containing an aluminum–selenium multiple bond and with 1,3,5,7-cyclooctatetraene (COT) to give the first aluminum complex containing a reduced COT-ligand with a strong aromatic character, respectively.<sup>12</sup> Both aluminyl anion complexes reacted with two abundant greenhouse gases (CO<sub>2</sub> and N<sub>2</sub>O) *via* cycloaddition to generate a monoalumoxane anion.<sup>13</sup> The first isolable example of a room temperature stable monomeric cyclopentadienylaluminum(I) derivative was reported by Braunschweig and co-workers, which was supported by a bulky 1,2,4-tri-*tert*-butylcyclopentadienyl (Cp<sup>3t</sup>) ligand (IV, Fig. 1).<sup>14a</sup> The same group also reported the first example of a monomeric Lewis base stabilized Al(I) hydride that can be isolated and handled under ambient conditions (V, Fig. 1).<sup>14b</sup> Very recently, Yamashita's group reported an alkyl-substituted aluminum anion that exhibits very strong basicity and nucleophilicity (VI, Fig. 1).<sup>14c</sup> These species have been observed to form both covalent and donor–acceptor bonds, revealing both the reducing and nucleophilic properties of these novel complexes.

Gallium(I) compounds are often driven by the thermodynamic preference for the metal center to exist in the +3 oxidation state. Having said this, much of the reported chemistry of monomeric gallium(I) compounds is derived from the significant basicity of the metal through its lone pair of electrons.

Gallium(I) compounds are generally more stable towards disproportionation than the corresponding aluminum(I) compounds. So far, several gallium(I) *N*-heterocycles have been reported.<sup>15,16</sup> Bi- and tridentate ligand systems have been used in the preparation of a variety of neutral and anionic gallium(I) heterocycles (*e.g.*, five-membered anionic complexes VII–VIII, a guanidinate complex IX and a monomeric tris(pyrazolylborate) complex X, see Fig. 2).<sup>16</sup> These compounds have been prepared either by salt-metathesis reactions between alkali metal salts of the ligands and “GaI” or by alkali metal reduction of Ga<sup>II</sup> or Ga<sup>III</sup> precursors. The monomeric example of Ga<sup>I</sup> amide (XI, Fig. 2) can be considered to be having a quasi one-coordinate metal center, which also exhibits weak intramolecular arene interactions in the solid state.<sup>16m</sup> Recently, a pincer-type gallylene ligand has been successfully synthesized utilizing bis(phosphino)-terpyridine as an efficient scaffold for the Ir–Ga<sup>I</sup> bond, which enabled various reactions at the Ir center by keeping the gallylene ligand intact.<sup>17</sup>

The β-diketiminato ligands typically provide monoanionic, bidentate support for metal complexes and offer a much higher degree of steric control through the choice of *N*-substituents. By tuning the steric and electronic properties of the supporting β-diketiminato ligands, the reactivity of the compounds can be significantly improved.<sup>18</sup> Thus, complexes with a low-valent metal could be stabilized by the employment of sterically encumbering β-diketiminato ligands. It is interesting to note that with a redox-inactive metal bound and appropriate substituents, β-diketiminato ligands become redox-active ligands.<sup>19</sup> Herein we present an overview that is of relevance to the corresponding bond

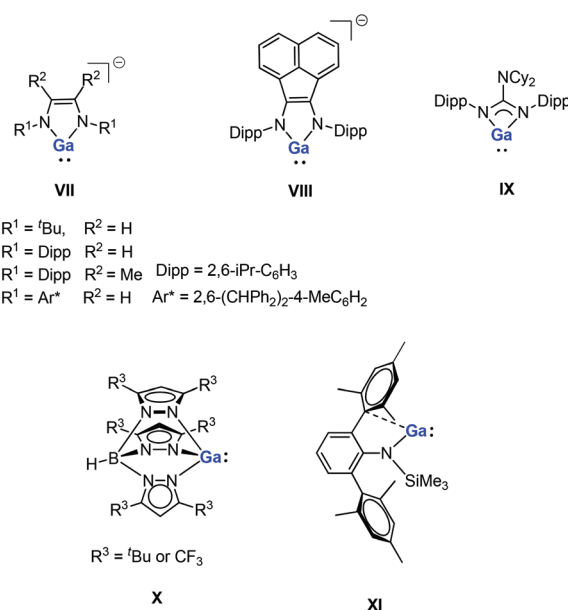


**Fig. 2** Reported examples of gallium(I) *N*-heterocycles.



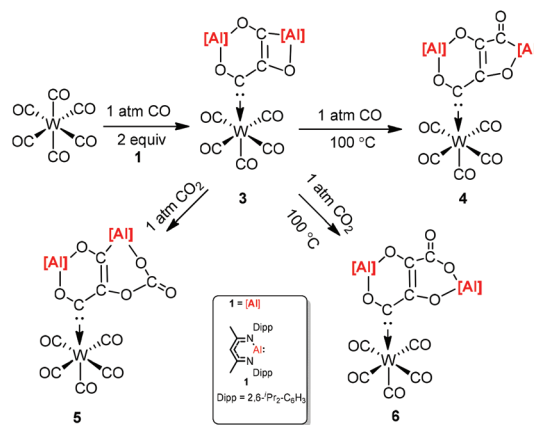
activation by aluminum(i) and gallium(i) with  $\beta$ -diketiminate ligands.

## 2. Chemistry of $\text{DippNacNacAl(i)}$ and $\text{DippNacNacGa(i)}$

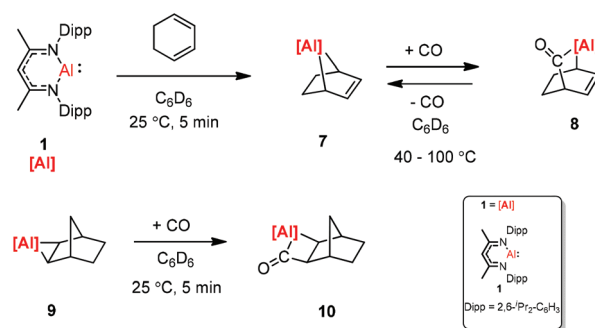
The monomeric aluminum carbenoid  $\text{DippNacNacAl(i)}$  (**1**) was prepared through reduction of the corresponding  $\text{DippNacNacAlI}_2$  with potassium (Scheme 1).<sup>8a</sup> At the same time, Power and co-workers reported a  $\beta$ -diketiminate stabilized Ga(i) monomer  $\text{DippNacNacGa(i)}$  (**2**) (Scheme 1).<sup>20</sup> It was obtained by the reaction of  $[\text{Li}\{\text{HC}(\text{CMeNDipp})_2\}]$  with “GaI”. The remarkable thermal stability of the compounds toward disproportionation reaction (decomp.  $>150^\circ\text{C}$ ) can be attributed to the steric bulk of the  $\beta$ -diketiminate ligand, which provides kinetic protection to the metal center. X-ray crystal structure analysis showed that compound **2** is monomeric and isostructural with its aluminum counterpart. With a singlet lone pair and formally empty p-orbital on the metal, the neutral heterocycles  $\text{DippNacNacAl(i)}$  and  $\text{DippNacNacGa(i)}$  have the potential to exhibit both nucleophilic and electrophilic characteristics.

### 2.1. Small-molecule activation

CO and  $\text{CO}_2$  activation by transition-metal complexes has been studied extensively for many years. However, the activation of CO and  $\text{CO}_2$  with Group 13 metal elements and their compounds has been explored scarcely.<sup>21</sup> In 2018, Crimmin *et al.* reported carbon chain growth from C1 to C3 and to C4 by sequential reactions of CO and  $\text{CO}_2$  with a transition metal carbonyl complex in the presence of an aluminum(i) complex (Scheme 2).<sup>22</sup> Warming a frozen suspension of  $[\text{W}(\text{CO})_6]$  with 2 equiv. of **1** under 1 atm of CO from  $-78^\circ\text{C}$  to r.t. in a benzene- $\text{d}_6$  solvent results in the formation of the C3 homologated product **3**. Heating the isolated and purified sample of **3** under one atmosphere of CO leads to the formation of the chain growth product **4**. Further chain growth of C3 to a C4 fragment could be achieved upon the reaction of **3** with one atmosphere of  $\text{CO}_2$ . Although the reaction of  $\text{CO}_2$  with **3** at  $25^\circ\text{C}$  initially produces **5**, when the sample **3** is heated at  $100^\circ\text{C}$  for 48 h, it completely converts to **6**. No reaction occurs between **1** and CO in the absence of  $[\text{W}(\text{CO})_6]$ . The gallium products of these reactions are not reported.



**Scheme 2** Carbon chain growth by sequential reactions of CO and  $\text{CO}_2$  with  $[\text{W}(\text{CO})_6]$  and **1**.



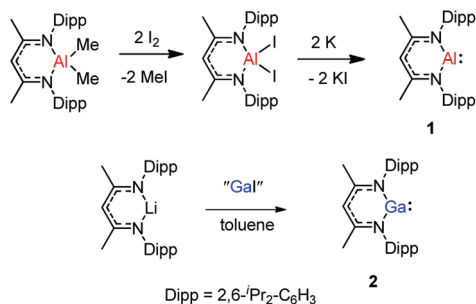
**Scheme 3** Syntheses of [2.2.1] metallobicycle **7** and reversible CO insertion.

The [2.2.1] metallobicyclic compound **7** was synthesized by the cycloaddition of complex (**1**) with low-valent aluminum and 1,3-cyclohexadiene. The exposure of a  $\text{C}_6\text{D}_6$  solution of **7** to one atmosphere of CO generated the insertion product **8**. As shown in Scheme 3 the reaction mixture is reversible, when **8** is heated for longer time. Compound **9** was also studied in the reaction with CO, and the insertion of CO into the Al–C bond was observed. However, compound **10** decomposes at  $25^\circ\text{C}$  within 12 h into an intractable mixture of products.<sup>23</sup>

Crimmin and co-workers documented the first reversible addition of ethylene to aluminum(i) **1**. The monomeric molecular aluminum(i) complex reacted with a series of terminal and strained alkenes including norbornene,<sup>24a</sup> ethylene, propylene, hex-1-ene, 3,3-dimethyl-1-butene, allylbenzene and 4-allylanisole. Remarkably all these reactions are reversible under mild conditions (Scheme 4).<sup>24b</sup>

### 2.2. Cleavage of the M–X single bond

Aluminum(i) **1** has been developed to act as a synthon for the preparation of aluminum–metal bonded compounds *via* oxidative insertion of the Al center into metal–halogen linkages. Jones *et al.* reported the first example of molecular complexes

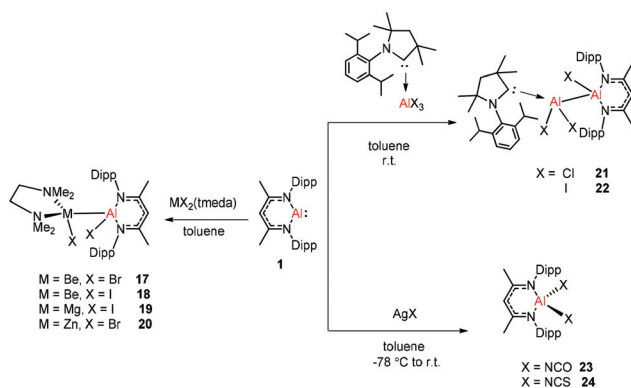


**Scheme 1** Syntheses of  $\text{DippNacNacAl(i)}$  and  $\text{DippNacNacGa(i)}$ .

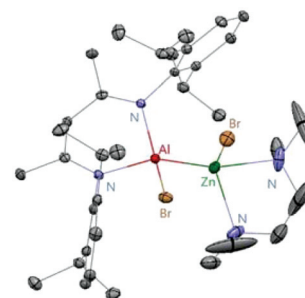


Scheme 4 Reversible alkene binding to 1.

containing an unsupported Be–Al bond. The Be–Al bonded complexes **17** and **18** were obtained as yellow crystalline solids from the reaction of  $\text{DippNacNacAl}(\text{I})$  (**1**) with  $[\text{BeX}_2(\text{tmeda})]$  ( $\text{X} = \text{Br}$  or  $\text{I}$ ,  $\text{tmeda}$  = tetramethylethylenediamine) in 1 : 1 stoichiometry (Scheme 5). The Be–Al bond distances in **17** and **18** are 2.474(1) Å and 2.432(6) Å, respectively. They are significantly longer than the sum of single bond covalent radii of the elements (2.28 Å). DFT calculations reveal that the compounds with metal–metal bonds have a high s-character. This is consistent with similar Pauling electronegativities between Al and Be. The isostructural Mg–Al (**19**) and Zn–Al (**20**) analogues of these complexes have been isolated in the 1 : 1 reaction of  $\text{DippNacNacAl}(\text{I})$  (**1**) with  $[\text{MgI}_2(\text{tmeda})]$  and  $[\text{ZnBr}_2(\text{tmeda})]$ , respectively (Scheme 5).<sup>25</sup> The composition of compound **20** was confirmed by means of single-crystal X-ray structural analysis (Fig. 3). Compound **20** has distorted tetrahedral Al and Zn centers. The Zn–Al bond distance is 2.471(1) Å, which is longer than the sum of covalent radii of the elements (2.44 Å).  $\text{DippNacNacGa}(\text{I})$  (**2**) shows no reactivity towards  $[\text{BeX}_2(\text{tmeda})]$ , even at elevated temperature. Roesky *et al.* reported unsymmetrical dialumanes by the disproportionation of  $\text{DippNacNacAl}(\text{I})$  (**1**) with  $(\text{Me}_2\text{cAAC})\text{AlX}_3$  ( $\text{X} = \text{Cl}$ ,  $\text{I}$ ) adducts (Scheme 5). The Al–Al bond lengths in compound **21** (2.6327(11) Å) and compound **22** (2.5953(16) Å) are slightly shorter than those of symmetric Al–Al bond lengths, owing to the relaxation of the electrostatic repulsion between the Al atoms.<sup>26</sup> The reactions



Scheme 5 Synthesis of compounds 17–24.

Fig. 3 X-ray single crystal structure of compound **20**.

of  $\text{DippNacNacAl}(\text{I})$  (**1**) with  $\text{AgX}$  ( $\text{X} = \text{OCN}$ ,  $\text{SCN}$ ) resulted in compounds **23** and **24** containing two pseudohalide groups coordinated to the aluminum(III) center.<sup>27</sup> The reactions proceed *via* oxidative addition of the pseudohalides and elimination of the silver metal.

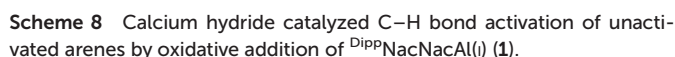
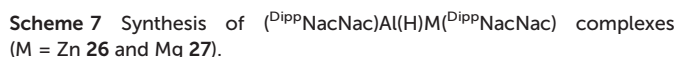
Harder *et al.* reported a combined attack of  $[(\text{DippNacNac})\text{Ca}^+(\text{C}_6\text{H}_6)][\text{B}(\text{C}_6\text{F}_5)_4]^-$  and  $\text{DippNacNacAl}(\text{I})$  (**1**), which led to the complete dearomatization of benzene to give  $\text{C}_6\text{H}_6^{2-}$  that chelates to the Al(III) center (Scheme 6).

The molecular structure of **25**, however, showed a heterobimetallic complex in which the  $\text{C}_6\text{H}_6^{2-}$  fragment is bridging to Ca and to the Al center.<sup>28a</sup> Crimmin *et al.* reported the first catalytic method for the transformation of C–H bonds in unactivated arenes (benzene, toluene and xylene) into C–Al bonds and proposed a mechanism by which the C–H bond is activated by an unusual Al–Pd intermetallic complex.<sup>28b</sup> Very recently, Harder *et al.* have described the stoichiometric reactions of  $\text{DippNacNacAl}(\text{I})$  (**1**) with  $[(\text{DippNacNac})\text{MgH}]_2$  and  $(\text{DippNacNac})\text{ZnH}$ , respectively in benzene, where the Al center inserts into the metal hydride bond, which results in  $(\text{DippNacNac})\text{Al}(\text{H})\text{M}(\text{DippNacNac})$  complexes ( $\text{M} = \text{Zn}$  **26**,  $\text{Mg}$  **27**) (Scheme 7).<sup>28c</sup> However, the reaction of the calcium hydride complex with **1** in benzene followed a different course leading to benzene C–H alumination. The cleavage of the  $\text{sp}^2$  C–H bond in unactivated arenes (benzene, toluene and xylene) by the low valent Al(I) complex **1** at room temperature has been achieved by the catalytic presence of  $[(\text{DippNacNac})\text{CaH}]_2$  (Scheme 8). The possible pathway is the combined action of nucleophilic Al and arene activation by  $\pi$ -coordination to a Lewis acidic Ca center, which is parallel to the first aluminyl anions.<sup>11c</sup>

Schulz *et al.* reported that a solution of  $\text{DippNacNacAl}(\text{I})$  (**1**) reacts with  $\text{E}_2\text{Et}_4$  ( $\text{E} = \text{Sb}$ ,  $\text{Bi}$ ) in toluene to insert  $\text{DippNacNacAl}(\text{I})$  (**1**) into the E–E bond with the formation of  $\text{DippNacNacAl}(\text{EET}_2)_2$

Scheme 6 Activation of benzene using Al(I) and  $\text{Ca}^{2+}$ .





$$\text{E} = \text{Sb} \quad \mathbf{34}$$

$$\text{Bi} \quad \mathbf{35}$$
  

$$\xrightleftharpoons{\text{E}_2\text{Et}_4}$$
  

$$\xleftarrow[\text{r.t., toluene}]{\text{E}_2\text{Et}_4} \quad \text{Ga(II) complex} \quad \text{M} = \begin{matrix} \text{Al} & \mathbf{1} \\ \text{Ga} & \mathbf{2} \end{matrix}$$
  

$$\xrightarrow[\text{hexane, r.t. to } 50^\circ\text{C}]{\text{BiOTf}_3} \quad \text{Ga(III) complex} \quad \begin{matrix} \text{Tf} = \text{SO}_2\text{CF}_3 & \mathbf{36} \\ \text{C}_6\text{F}_5 & \mathbf{37} \end{matrix}$$
  

$$\xrightarrow[\text{80 } ^\circ\text{C}]{\text{toluene, BiEt}_3} \quad \text{Ga(III) complex} \quad \begin{matrix} \text{M} = \text{Al} & \mathbf{38} \\ \text{Ga} & \mathbf{39} \end{matrix}$$

**Scheme 9** Cleavage of Sb–Sb and Bi–Bi bonds by  $\text{Dipp}^{\text{Nac}}\text{NacAl}(\text{I})$  and  $\text{Dipp}^{\text{Nac}}\text{NacGa}(\text{I})$ , respectively.

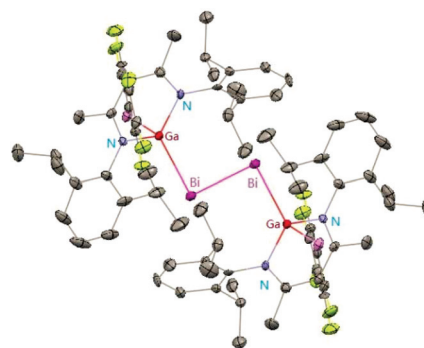


**Fig. 4** X-ray single crystal structure of compound **36**.

(Scheme 9). The consecutive second activation proceeds at a higher temperature through the reductive elimination of  $\text{Dipp}^{\text{Nac}}\text{NacMet}_2$ , elemental Bi and  $\text{BiEt}_3$ .<sup>31</sup>

Heavy-metal complexes containing gallium-lead and gallium-mercury bonds were derived from the oxidative addition of  $\text{D}^{\text{ipp}}\text{NacNacGa(I)}$  (**2**) with the corresponding metal precursors. The reaction of  $\text{Me}_3\text{PbCl}$  with  $\text{D}^{\text{ipp}}\text{NacNacGa(I)}$  (**2**) in THF at ambient temperatures afforded compound  $\{[(\text{D}^{\text{ipp}}\text{NacNac})\text{Ga}(\text{Cl})]\text{PbMe}_3\}$  (**40**) in high yield. In addition, the reaction between  $[\text{Pb}(\text{OSO}_2\text{CF}_3)_2]$  and  $\text{D}^{\text{ipp}}\text{NacNacGa(I)}$  (**2**) (two equiv.) leads to the complex **41** containing a Ga-Pb<sup>II</sup>-Ga linkage (Fig. 5). When two equiv. of  $\text{D}^{\text{ipp}}\text{NacNacGa(I)}$  (**2**) were treated with  $[\text{Pb}(\text{OSO}_2\text{CF}_3)_2 \cdot 2\text{H}_2\text{O}]$  in THF, deep red crystals of **42** were formed in very poor yield (Scheme 10). The structure of the compound consists of a bent Ga-Pb-Ga backbone with a bridging triflate group between the Ga-Pb bond and a

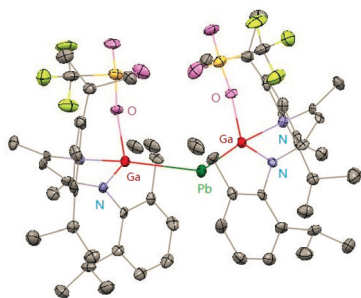
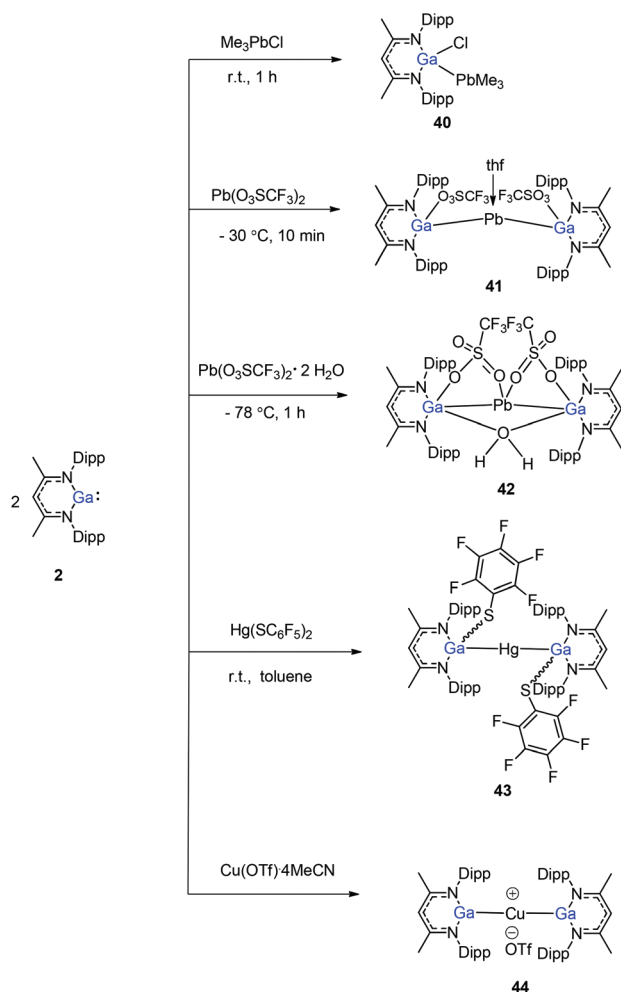


Fig. 5 X-ray single crystal structure of compound **41**; the THF molecule attached to lead is omitted for clarity.

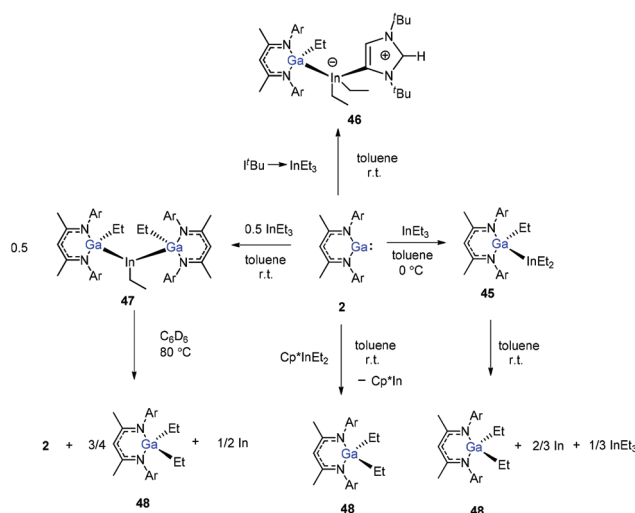


Scheme 10 The oxidative addition of Pb/Hg/Cu salts to  $\text{DippNacNacGa(I)}$  (**2**).

weakly interacting water molecule at the gallium center. Similarly, the reaction of mercury thiolate  $\text{Hg}(\text{SC}_6\text{F}_5)_2$  with  $\text{DippNacNacGa(I)}$  (**2**) (two equiv.) produced the bimetallic homoleptic compound **43** (Scheme 10).<sup>32</sup> The linear cationic complex  $[\{(\text{DippNacNacGa})_2\text{Cu}\}[\text{OTf}]\cdot 2\text{C}_6\text{H}_5\text{F}$  (**44**,  $\text{Tf} = \text{SO}_2\text{CF}_3$ ) was obtained from the reaction of  $\text{DippNacNacGa(I)}$  (**2**) (two equiv.) with  $\text{Cu}(\text{OTf})\cdot 4\text{CH}_3\text{CN}$ .<sup>33</sup>

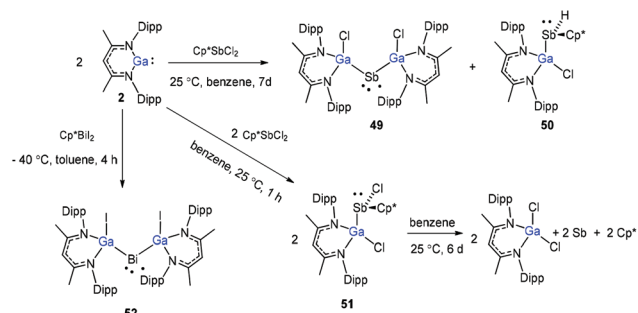
In addition, Schulz *et al.* showed that  $\text{DippNacNacGa(I)}$  (**2**) inserted into the In–C bond of  $\text{InEt}_3$  resulted in the formation of  $\text{DippNacNacGaEt}(\text{InEt}_2)$  (**45**). The solution of **45** in benzene and toluene tends to decompose slowly at ambient temperature. But the reaction of  $\text{DippNacNacGa(I)}$  (**2**) with  $\text{I}^t\text{Bu} \rightarrow \text{InEt}_3$  [ $\text{I}^t\text{Bu} = [\text{C}(\text{N}^t\text{Bu}_2\text{CH})_2]$ ] resulted in a stable compound **46**, where the carbene coordinates to the indium atom. The reaction of  $\text{InEt}_3$  with 2 equiv. of  $\text{DippNacNacGa(I)}$  (**2**) resulted in a double insertion product  $[\text{DippNacNacGa}(\text{Et})_2]\text{InEt}$  (**47**) (Scheme 11), while further insertion of  $\text{DippNacNacGa(I)}$  (**2**) into the remaining In–Et bond does not occur. Complex **57** gradually decomposes at 80 °C in  $\text{C}_6\text{D}_6$ , resulting in  $\text{DippNacNacGa}$  (**2**) and  $\text{DippNacNacGaEt}_2$  (**48**). A similar reaction between  $\text{DippNacNacGa(I)}$  (**2**) and  $\text{Cp}^*\text{InEt}_2$  ( $\text{Cp}^* = \text{C}_5\text{Me}_5$ ) leads to the production of  $\text{DippNacNacGaEt}_2$  (**48**). These reactions proceeded *via* the oxidation of  $\text{DippNacNacGa(I)}$  (**2**) with the In–Et bond and subsequent reductive elimination of  $\text{DippNacNacGaEt}_2$  from the indium(III) center.<sup>35</sup>

Schulz and co-workers have also reported a stibinyl radical  $[\text{DippNacNac}(\text{Cl})\text{Ga}]_2\text{Sb}^\bullet$  (**49**) by the reaction of two equiv. of  $\text{DippNacNacGa(I)}$  (**2**) with  $\text{Cp}^*\text{SbCl}_2$  (Scheme 12), and the traces of  $\text{DippNacNac}(\text{Cl})\text{GaSb}(\text{H})\text{Cp}^*$  (**50**) were formed as a byproduct. Similarly, the equimolar reaction yielded  $\text{DippNacNac}(\text{Cl})\text{GaSb}(\text{Cl})\text{Cp}^*$  (**51**), which slowly decomposed to  $\text{DippNacNacGaCl}_2$ , decamethylfulvalen ( $\text{Cp}^*_2$ ) and the antimony metal. The analogous reaction of  $\text{DippNacNacGa(I)}$  (**2**) with  $\text{Cp}^*\text{BiI}_2$  yielded a bis-muthinyl radical  $[\text{DippNacNac}(\text{I})\text{Ga}]_2\text{Bi}^\bullet$  (**52**) (Scheme 12). Their formation illustrates the stepwise insertion of  $\text{DippNacNacGa(I)}$  (**2**) into the E–X bond of  $\text{Cp}^*\text{EX}_2$  followed by the homolytic bond cleavage of the E– $\text{Cp}^*$  bond and elimination of  $\text{Cp}^*_2$ . Theoretical calculations showed the significant electron delocalization of the Sb and Bi unpaired radicals onto the Ga ligands. Compounds **49** and **52** adopt V-shaped geometries with Ga–E–Ga bond angles of 104.89(1)° (**49**) and 106.68(3)° (**52**), respectively. Compound **53** was isolated by the direct reaction of **49** with  $\text{KC}_8$  in benzene, which gives the first struc-

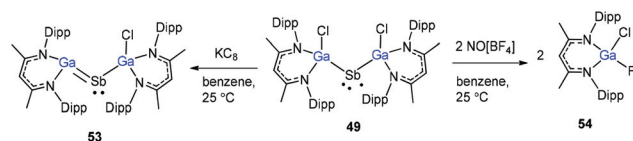


Scheme 11 Syntheses and thermal stability of compounds **45**–**48**.





Scheme 12 Synthesis of compounds 49–52.



Scheme 13 Single-electron oxidation and reduction reactions of compound 49.

turally characterized compound containing a Ga=Sb double bond (Scheme 13). In contrast, the equimolar redox reaction of 2 with the single-electron oxidant  $[\text{NO}][\text{BF}_4]$  occurred with the formation of  $^{\text{Dipp}}\text{NacNacGaClF}$  (54).<sup>36</sup>

The  $\text{Cp}^*\text{AsCl}_2$  ( $\text{Cp}^* = \text{C}_5\text{Me}_5$ ) reacted with one equiv. of  $^{\text{Dipp}}\text{NacNacGa(I)}$  (2) with the insertion of  $^{\text{Dipp}}\text{NacNacGa(I)}$  (2) into one As–Cl bond and the subsequent formation of  $^{\text{Dipp}}\text{NacNac(Cl)GaAs(Cl)Cp}^*$  (55) (Scheme 14). In contrast, the reaction of two equiv. of  $^{\text{Dipp}}\text{NacNacGa(I)}$  (2) with  $\text{Cp}^*\text{AsCl}_2$  proceeds with the formation of gallaarsene  $^{\text{Dipp}}\text{NacNacGaAsCp}^*$  (56) with a Ga=As double bond and  $(^{\text{Dipp}}\text{NacNacGaCp}^*)(^{\text{Dipp}}\text{NacNacGa})(\eta^1, \eta^2, \mu\text{-As}_3)$  (57), containing a central GaAs<sub>3</sub> butterfly type core. The central structural motif of 57 is the bridging As<sub>3</sub> three-membered ring, which coordinates in an  $\eta^1$  and  $\eta^2$  fashion to two Ga atoms, respectively (Fig. 6).<sup>37</sup>

To evaluate the reduction potential of  $^{\text{Dipp}}\text{NacNacGa(I)}$  (2) in detail, Schulz *et al.* studied the reactions of  $^{\text{Dipp}}\text{NacNacGa(I)}$  (2) with other  $\text{Sb}^{\text{III}}$  reagents.  $^{\text{Dipp}}\text{NacNacGa(I)}$  (2) reacted with  $\text{SbX}_3$  ( $\text{X} = \text{NMe}_2, \text{Cl}$ ) in a 2 : 1 molar ratio to form Ga-substituted distibenes  $[(^{\text{Dipp}}\text{NacNacGaX})_2\text{Sb}_2]$  ( $\text{X} = \text{NMe}_2$  58, Cl 59)

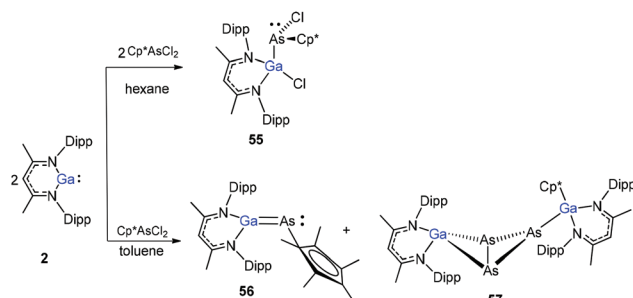
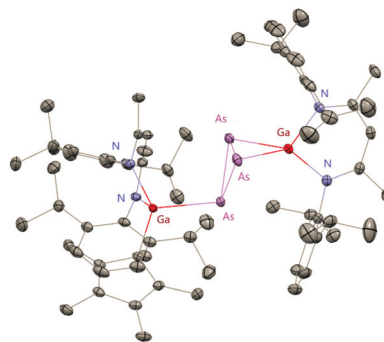
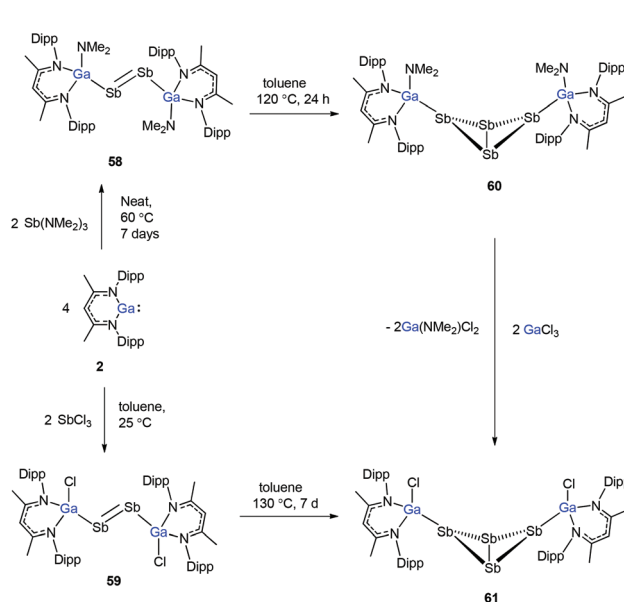
Scheme 14 The reaction of  $^{\text{Dipp}}\text{NacNacGa(I)}$  (2) with  $\text{Cp}^*\text{AsCl}_2$ .

Fig. 6 X-ray single crystal structure of compound 57.



Scheme 15 Syntheses of compounds 58–61.

(Scheme 15). Heating a toluene solution of 58 at 120 °C for 24 h yielded  $[(^{\text{Dipp}}\text{NacNacGaNMe}_2)_2(\mu, \eta^{1:1}\text{-Sb}_4)]$  (60). But complex 59 required 7 days of heating at 130 °C to give  $[(^{\text{Dipp}}\text{NacNacGaCl})_2(\mu, \eta^{1:1}\text{-Sb}_4)]$  (61). Compound 58 can react with  $\text{GaCl}_3$  to form 59; in addition, 59 reacts with Li amide to form 58. The central  $\text{Sb}_4$  unit in 60 and 61 adopts a butterfly type conformation (Fig. 7). Interestingly, compound 60 reacted with  $\text{GaCl}_3$  in an amide/Cl exchange reaction with the subsequent formation of 61.<sup>38</sup>

To better understand the reaction mechanism leading to compounds containing  $\text{Sb}=\text{Sb}$  and  $\text{Ga}=\text{Sb}$  double bonds, the reactions of  $\text{SbCl}_3$  with different equiv. of  $^{\text{Dipp}}\text{NacNacGa(I)}$  (2) at different temperatures were investigated. The  $^{\text{Dipp}}\text{NacNacGaSbGa(X)}^{\text{Dipp}}\text{NacNac}$  ( $\text{X} = \text{F}$  62, Cl 63, Br 64, and I 65) compounds were formed by a twofold insertion of  $^{\text{Dipp}}\text{NacNacGa(I)}$  (2) into two Sb–X bonds, followed by an intramolecular elimination of  $^{\text{Dipp}}\text{NacNacGaX}_2$  (Scheme 16). The reactions of two equiv. of  $^{\text{Dipp}}\text{NacNacGa(I)}$  (2) with  $\text{SbCl}_3$  at 8 °C yielded cyclotristibine 66. The Sb–Sb bond (2.8205(3)–2.8437(3) Å) in cyclotristibine 66 is typical of the Ga–Sb single bond.<sup>39</sup>

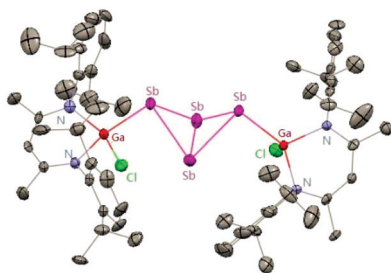
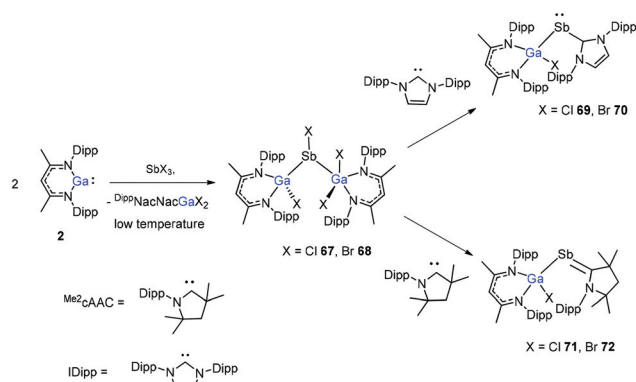


Fig. 7 X-ray single crystal structure of compound 61.



Scheme 16 Syntheses of gallastibenes containing Ga=Sb double bonds and cyclotristibine.

The insertion reactions of two equiv. of  $^{\text{Dipp}}\text{NacNacGa}(\text{I})$  (**2**) with  $\text{SbX}_3$  ( $\text{X} = \text{Cl}, \text{Br}$ ) at low temperature produced a double-inserted product  $(^{\text{Dipp}}\text{NacNacGaX})_2\text{SbX}$  ( $\text{X} = \text{Cl}$  **67**, Br **68**). In addition, the reaction of isolated compounds **67** and **68** with strong  $\sigma$ -donating carbenes (IDipp(1,3-bis-(2,6-diisopropyl-phenyl)imidazol-2-ylidene),  $\text{Me}_2\text{cAAC}$ ) yielded four carbene-stabilized stibinidenes (**69–72**) (Scheme 17). The studies reveal that IDipp-stabilized stibinidenes **69** and **70** show  $\text{Sb}-\text{C}_{\text{carbene}}$  single bonds, whereas the  $\text{Me}_2\text{cAAC}$ -stabilized derivatives **71** and **72** exhibit  $\text{Sb}-\text{C}_{\text{carbene}}$   $\pi$ -backbonding character.<sup>40</sup>



Scheme 17 Syntheses of IDipp- (**69** and **70**) and  $\text{Me}_2\text{cAAC}$ -stabilized stibinidenes (**71** and **72**).



Scheme 18 Syntheses of complexes **73** and **74**.

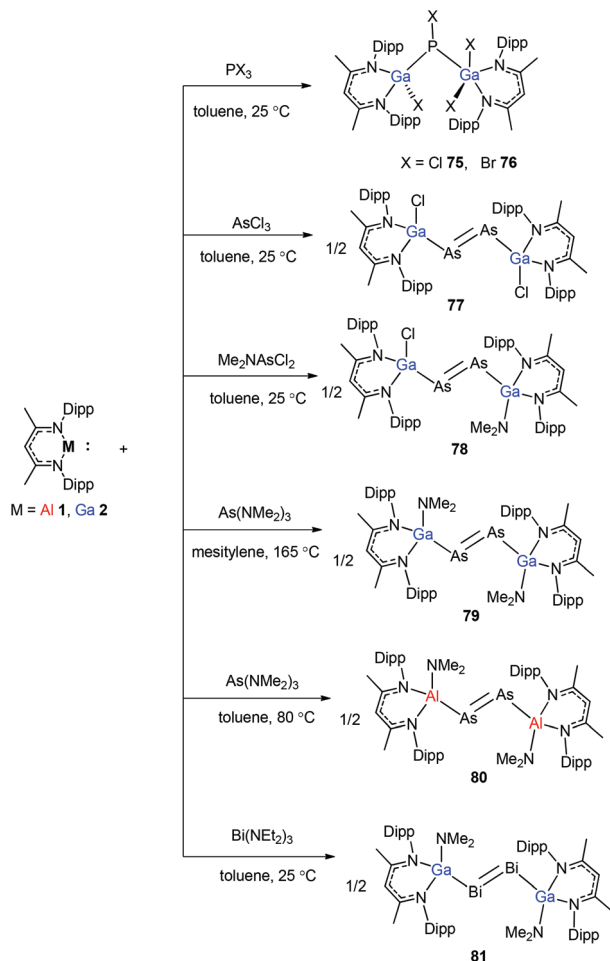
A red-brown complex **73** was obtained by the reaction of the half-sandwich complex  $[\text{Cp}^{\text{R}'}\text{Ni}(\mu\text{-Br})_2]$  ( $\text{Cp}^{\text{R}'} = \text{C}_5(\text{C}_6\text{H}_4\text{-4-Et})_5$ ) with  $^{\text{Dipp}}\text{NacNacGa}(\text{I})$  (**2**) in THF (Scheme 18).<sup>41</sup> The  $\text{Cp}^{\text{R}'}$ (centroid)-Ni-Ga linkage is bent, and the nickel atom is surrounded by an  $\eta^5$ -coordinated  $\text{Cp}^{\text{R}'}$  ligand and a  $\sigma$ -coordinated  $\text{Ga}(^{\text{Dipp}}\text{NacNac})$  ligand, while the bromide bridges the Ni-Ga bond. The reduction of **73** with  $\text{KC}_8$  afforded compound **74** where the " $\text{Cp}^{\text{R}'}\text{Ni}(\text{I})$ " fragment is trapped by  $^{\text{Dipp}}\text{NacNacGa}$ . The reduction of  $[\text{Cp}^{\text{R}'}\text{Ni}(\mu\text{-Br})_2]$  with  $\text{KC}_8$  and the subsequent addition of  $^{\text{Dipp}}\text{NacNacGa}(\text{I})$  (**2**) also result in compound **74** albeit in smaller yield (Scheme 18).

### 2.3. Cleavage of E'-E single and E'=E double bonds

To stabilize Ga-coordinated dipnictenes of the type  $[\text{DippNacNac}(\text{X})\text{Ga}]_2\text{E}_2$  ( $\text{E} = \text{P-Bi}$ ), the reactions of  $^{\text{Dipp}}\text{NacNacGa}(\text{I})$  (**2**) with phosphorus, arsenic, and bismuth halides and amides were studied.<sup>42</sup> Two equiv. of  $^{\text{Dipp}}\text{NacNacGa}(\text{I})$  (**2**) reacted with  $\text{PX}_3$  ( $\text{X} = \text{Cl}, \text{Br}$ ) in toluene at ambient temperature with the insertion of  $^{\text{Dipp}}\text{NacNacGa}(\text{I})$  (**2**) into two P-X bonds, which resulted in  $[\text{DippNacNac}(\text{X})\text{Ga}]_2\text{PX}$  ( $\text{X} = \text{Cl}$  **75**, Br **76**) (Scheme 19). Similar twofold insertion reactions into  $\text{AsCl}_3$  and the subsequent elimination of  $^{\text{Dipp}}\text{NacNacGaCl}_2$  resulted in the formation of the stable Ga-coordinated diarsene species, which was isolated as a green crystalline solid **77** (Scheme 20). The analogous reaction with  $\text{Me}_2\text{NASCl}_2$  yielded unsymmetrically-substituted diarsene  $[\text{DippNacNac}(\text{Cl})\text{Ga}]\text{As}=\text{As}[\text{Ga}(\text{NMe}_2)^{\text{Dipp}}\text{NacNac}]$  (**78**) (Scheme 20). In contrast, the reaction of  $^{\text{Dipp}}\text{NacNacGa}(\text{I})$  (**2**) with  $\text{As}(\text{NMe}_2)_3$  required much harsher reaction conditions. A mixture of  $^{\text{Dipp}}\text{NacNacGa}(\text{I})$  (**2**) and  $\text{As}(\text{NMe}_2)_3$  heated at  $165^\circ\text{C}$  for 5 days resulted in compound **79** (Scheme 19). Its analogous reaction with  $^{\text{Dipp}}\text{NacNacAl}(\text{I})$  (**1**) yielded  $[\text{DippNacNac}(\text{Me}_2\text{N})\text{Al}]_2\text{As}_2$  (**80**) after heating at  $80^\circ\text{C}$  for one day (Scheme 20). Finally, the reaction of  $^{\text{Dipp}}\text{NacNacGa}(\text{I})$  (**2**) with  $\text{Bi}(\text{NET}_2)_3$  also occurred with the insertion and elimination of  $^{\text{Dipp}}\text{NacNacGa}(\text{NET}_2)_2$  and resulted in the corresponding Ga-substituted dibismuthene  $[\text{DippNacNac}(\text{Et}_2\text{N})\text{Ga}]_2\text{Bi}_2$  (**81**) (Scheme 19). The reaction of **2** with elemental tellurium yielded the Te-bridged compound  $[\text{DippNacNacGa}-\mu\text{-Te}]_2$  (**82**).







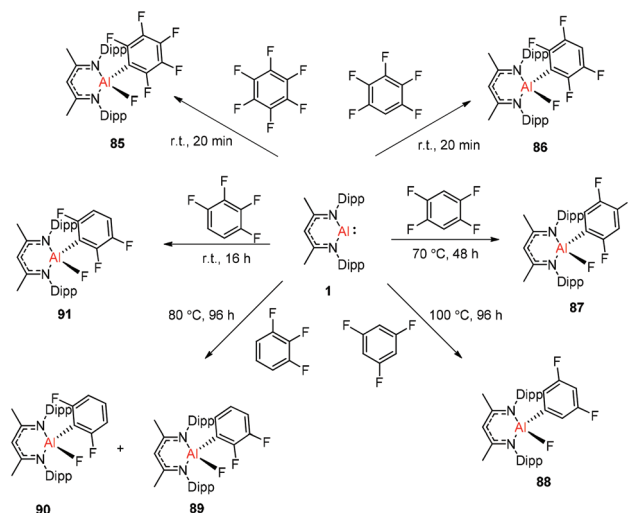
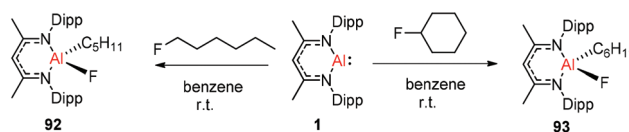
Scheme 19 Syntheses of complexes 75–81.

Scheme 20 Te–Te and Te–C bond cleavage reactions using  $\text{DippNacNacGa(i)}$  (2).

Moreover, the cleavage of the Te–Te and Te–C bonds upon reactions of 2 with  $\text{Ph}_2\text{Te}_2$  and  $i\text{Pr}_2\text{Te}$  resulted in the formation of  $\text{DippNacNacGa}(\text{TePh})_2$  (83) and  $\text{DippNacNacGa}(i\text{Pr})\text{Te}(i\text{Pr})$  (84), respectively (Scheme 20).<sup>34</sup>

Nikonov and Crimmin groups separately reported the reactions of the monomeric  $\text{Al(i)}$  complex with various fluoroalkenes and fluoroarenes, resulting in the breaking of strong  $\text{sp}^2$  and  $\text{sp}^3$  C–F bonds. Aluminum(i) compound 1 undergoes a facile oxidative addition with aryl C–F bonds.<sup>43</sup> The reaction of 1 with an excess of hexafluorobenzene or pentafluorobenzene resulted in compounds 85 and 86, respectively (Scheme 21). A further decrease in the number of fluorine atoms in the starting arene necessitates an increase in the reaction temperature to cleave the C–F bond. The cleaving ability decreases in the order  $o- > p- > m-$ . The addition of 1-fluorohexane or fluorocyclohexane to 1 at room temperature yielded the corresponding aluminum alkyl 92 and 93, respectively (Scheme 22).<sup>43a</sup> The reaction with (*E*)-1,3,3,3-tetrafluoro-propene(HFO-1234ze) resulted in the immediate formation of a 4 : 1 mixture of 94-*E* and 94-*Z* (Scheme 23). The addition of hexafluoropropene to 1 gave two products which were separated by fractional crystallization from hexane. 95 is formed from the internal  $\text{sp}^2$  C–F bond cleavage, while 96 is the result of breaking the terminal  $\text{sp}^2$  C–F bond *trans* to the  $\text{CF}_3$  group. The reaction of 1 with 3,3,3-trifluoropropene yielded 97 by the formation of a metal-cyclopropane intermediate followed by  $\beta$ -fluoride elimination (Scheme 23).<sup>24a</sup>

Streubel and co-workers described the reaction of monovalent compounds  $\text{DippNacNacM}$  ( $M = \text{Al}$ ,  $\text{Ga}$ ) with imidazole-2-thione based tricyclic 1,4-diphosphine, which produced the corresponding 7-metalla-1,4-diphosphanorbornadiene (98, 99) (Scheme 24).<sup>44a</sup> Previously Nikonov *et al.* described the oxi-

Scheme 21 Oxidation addition of  $\text{C}(\text{sp}^2)\text{–F}$  bonds by 1.Scheme 22 Oxidation addition of  $\text{C}(\text{sp}^3)\text{–F}$  bonds to 1.



**Scheme 23** Reactions of **1** with (*E*)-1,3,3,3-tetrafluoropropene, hexafluoropropene and trifluoropropene, respectively.



**Scheme 24** Reaction of tricyclic 1,4-diphosphinine with  $\text{DippNacAl(i)}$  (**1**) and  $\text{DippNacGa(i)}$  (**2**) to get 7-metalla-1,4-diphosphanorbornadienes **98** and **99**.

ductive cleavage of the C=S bond at the metal center,<sup>44b</sup> while **98** and **99** undergo the [4 + 1] cycloaddition reaction, which is both kinetically and thermodynamically favorable.

The aluminum(i) compound  $\text{DippNacAl(i)}$  (**1**) reacted with diethyl sulfide at 50 °C, which resulted in the oxidative addition of the  $\text{C(sp}^3\text{)}\text{-S}$  bond. This is the first example of  $\text{C(sp}^3\text{)}\text{-S}$  bond activation by a main-group element.<sup>45</sup> The groups of Nikonov, Crimmin, and Kinjo independently reported the reactions of monomeric Al(i) compound **1** towards C–O bonds. The oxidative addition reaction of tetrahydrofuran with  $\text{DippNacAl(i)}$  (**1**) smoothly occurred at room temperature to give complex **101**,<sup>43b</sup> while the reaction between **1** and benzofuran upon heating at 80 °C slowly converted it to product **102**.<sup>43a</sup> The reaction of **1** with an equiv. amount of  $\text{L}'_2\text{PhB}$  (**103**) ( $\text{L}' = \text{oxazol-2-ylidene}$ ) in toluene instantly occurred with the insertion of  $\text{DippNacAl(i)}$  (**1**) into the C–O bond, affording complex **104** involving an Al, N, and O mixed heterocyclic carbene or anionic (amino)(boryl) carbene derivative (Scheme 25).<sup>46</sup>

Treatment of  $\text{DippNacAl(i)}$  (**1**) with thiourea resulted in the first carbene-stabilized terminal aluminum sulfide complexes **105** and **106** by the oxidative cleavage of the C=S bond. In contrast, the mixing of compound **1** and triphenyl-



**Scheme 25** C–O and C–S bond activation, respectively, by the aluminum(i) compound.

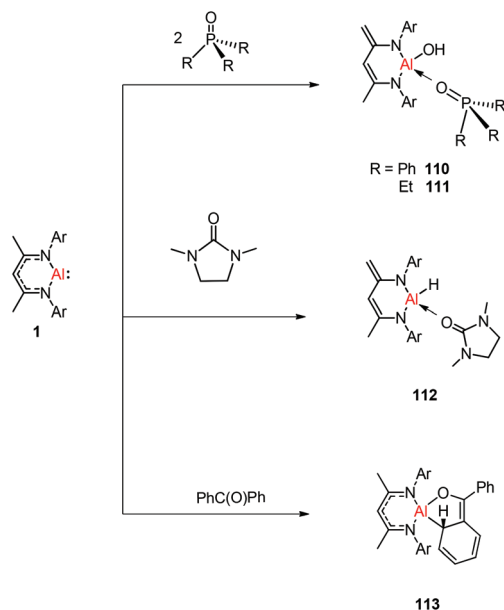
phosphine sulfide in a 1 : 1 ratio afforded a mixture of terminal sulfide  $\text{DippNacAl}=\text{S}(\text{S=PPh}_3)$ , unreacted **1**, and free triphenylphosphine. The existence of the Al–S double bond in **105** and **106** was supported by DFT calculations. Complex **105** undergoes facile cycloaddition with phenyl isothiocyanate to form compound **107** along with zwitterion **108** obtained from the coupling between the liberated carbene and  $\text{PhN}=\text{C}=\text{S}$  (Scheme 26).<sup>44b</sup> To investigate the oxidative cleavage of the unsaturated bond of the C=N unit, the reaction of  $\text{DippNacAl(i)}$  (**1**) with cyclic guanidine was accomplished and showed the unprecedented cleavage of the C–N multiple bond to give the carbene-ligated amido complex  $\text{DippNacAl}(\text{NHTol})(\text{SIME})$  ( $\text{SIME} = \text{C}\{\text{N}(\text{Me})\text{CH}_2\}_2$ ) (**109**). The splitting of the C=N bond in **109** is the first example of the oxidative addition of the C=N double bond to any metal center.<sup>47</sup> The DFT study supported that the production of **109** occurs *via* an intermediate of aluminum imide as a result of the oxidative cleavage of  $\text{ToIN}=\text{SIME}$  ( $\text{SIME} = \text{C}\{\text{N}(\text{Me})\text{CH}_2\}_2$ ) by **1**. The reactions of phosphine oxides with **1** occurred readily with the formation of hydroxyl derivatives  $\text{DippNacAl}(\text{OH})(\text{O}=\text{PR}_3)$  ( $\text{R} = \text{Ph}$  **110**,  $\text{Et}$  **111**). The C=O bond ( $179 \text{ kcal mol}^{-1}$ ) is much stronger when compared with the P=O bond ( $110 \text{ kcal mol}^{-1}$ ). Therefore, the reaction of cyclic urea 1,3-dimethyl-2-imidazolidinone with **1** resulted in an unexpected aluminum hydride  $\text{DippNacAlH}(\text{O}=\text{SIME})$  ( $\text{SIME} = \text{C}\{\text{N}(\text{Me})\text{CH}_2\}_2$ ) **112**, with the deprotonation of the weakly acidic methyl group in the backbone of the  $\text{DippNac}$  ligand.<sup>48a</sup> In contrast, the reactivity of **1** towards benzophenone afforded a ketyl species  $\text{NacAl}(\eta^2(\text{C},\text{O})\text{-OCPh}_2)$  (**113**) (Scheme 27). The latter compound undergoes easy cyclization reaction with an unsaturated substrate.<sup>48b</sup>

Recently Stephan *et al.* have reported the first heteroaluminirenes  $\text{DippNacAl}[\text{C}(\text{R})=\text{P}]$  ( $\text{R} = \text{'Bu}$  or adamantyl) **114** and **115** *via* the [1 + 2] cycloaddition reaction of the aluminum(i) complex  $\text{DippNacAl(i)}$  (**1**) with phosphalkynes, which feature moderate three-centered  $2\pi$ -electron aromaticity





**Scheme 26** Reactivity of **1** toward compounds with C=S and C=N unsaturated bonds.



**Scheme 27** Reactivity of **1** toward compounds with P=O and C=O unsaturated bonds.

(Scheme 28). The compounds containing the AlCP ring can be used as synthons to prepare a series of unprecedented Al- and P-containing heterocyclic frameworks.<sup>49</sup>

The Ga(I) compound easily undergoes cyclization with methacrolein at room temperature within 10 min to give gallium enolate **116**. Unlike the aluminum congener **1**, the gallium compound **2** does not cleave the P=S bond of



**Scheme 28** Synthesis of phosphaaluminirenes **114** and **115**.

Et<sub>3</sub>P=S, even upon heating to 80 °C. With Ph<sub>3</sub>P=S, however, a slow reaction occurs upon heating to 80 °C to obtain the sulfide (D<sup>i</sup>PPNacNacGa-S)<sub>2</sub> (**117**). Nevertheless, compound **2** readily reacts with two equiv. of PhNCS to give product **118** via C=S bond cleavage and cyclization, and also the dimer (D<sup>i</sup>PPNacNacGa)<sub>2</sub>(μ-S)(μ-CNPh) (**119**) at a ratio of 5 : 1 (3,5-Me<sub>2</sub>C<sub>6</sub>H<sub>3</sub>)NCO and PhNCO, respectively, reacts with **2**, readily to form the coupling products **120** and **121**. 1,3-Di-*p*-tolylcarbo-diimide and D<sup>i</sup>PPNacNacGa(I) formed the coupling product **122** (Scheme 29).<sup>50</sup>

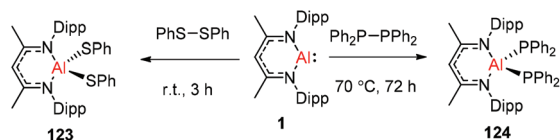
D<sup>i</sup>PPNacNacAl(I) (**1**) reacted with diphenyl disulfide to afford the symmetrically substituted bis(phenyl sulfide) aluminum complex **123** via the cleavage of the S-S bond in diphenyl disulfide. In a similar fashion, the reaction of **1** with bulky tetraphenyl diphosphine resulted in the cleavage of the P-P bond over the course of 3 d at 70 °C to produce the novel aluminum bis(diphenyl phosphido) complex (**124**) (Scheme 30).<sup>45</sup>

## 2.4 H-X bond activation

In 2014, Nikonov *et al.* reported the first examples of oxidative addition of a series of robust H-X bonds (X = H, B, C, Si, N, P, O) to a single Al(I) center. The addition of H<sub>3</sub>SiPh, HBPIn, HPPPh<sub>2</sub>,



**Scheme 29** Reactivity of **2** toward compounds with unsaturated bonds.



Scheme 30 P–P and S–S bond cleavage by 1.

$\text{HO}^i\text{Pr}$ ,  $\text{H}_2\text{NtBu}$  and  $\text{H}_2\text{NPh}$  with **1** proceeded smoothly at ambient temperature, while the reaction of bulkier silane ( $\text{H}_2\text{SiMePh}$ ),  $\text{H}_2$ ,  $\text{Cp}^*\text{H}$  with compound **1** required heating at 70 °C. The Al(i) compound reactivity toward the oxidative addition of  $^{\text{Dipp}}\text{NacNacAlH}_2$  is reversible, proving the possibility of reductive elimination from the species  $^{\text{Dipp}}\text{NacNacAlH}(X)$  ( $X = \text{H}, \text{B}, \text{C}, \text{Si}, \text{N}, \text{P}, \text{O}$ ).<sup>51</sup> Linti *et al.* described that  $^{\text{Dipp}}\text{NacNacGa(i)}(2)$  undergoes facile oxidative addition reactions towards  $\text{H}_2$ ,  $\text{HSnPh}_3$ ,  $\text{HNEt}_2$ ,  $\text{HPPH}_2$ ,  $\text{HOEt}$  and  $\text{H}_2\text{O}$ , leading to a series of gallium hydrides,  $^{\text{Dipp}}\text{NacNacGaH}(X)$  ( $X = \text{H}, \text{Sn}, \text{O}, \text{N}, \text{P}$ ), substituted by hydride, tin, alkoxy, amido and phosphido groups.<sup>52</sup> The oxidative addition of  $^{\text{Dipp}}\text{NacNacGa(i)}(2)$  with  $\text{HCCCH}_2\text{OH}$ ,  $\text{Ph}_2\text{Si}(\text{OH})_2$ ,  $(n\text{BuO})_2\text{P}(\text{O})(\text{OH})$  and  $(4\text{-Me-C}_6\text{H}_4\text{S}(\text{O})_2(\text{OH}))$  resulted in the formation of compounds  $^{\text{Dipp}}\text{NacNacGa}(\text{H})(\mu\text{-O})\text{CH}_2\text{CCH}$  (**138**),  $^{\text{Dipp}}\text{NacNacGa}(\text{H})(\mu\text{-O})\text{SiPh}_2(\text{OH})$  (**139**),  $^{\text{Dipp}}\text{NacNacGa}(\text{H})(\mu\text{-O})\text{P}(\text{O})(\text{O}^i\text{Bu})_2$  (**140**) and  $^{\text{Dipp}}\text{NacNacGa}(\text{H})(\mu\text{-O})\text{S}(\text{O})_2(\text{C}_6\text{H}_4\text{-4-Me})$  (**141**), respectively at very low temperature (Scheme 31).<sup>53</sup> Very recently, Nikonov *et al.* have reported the *in situ* oxidation of  $^{\text{Dipp}}\text{NacNacGa(i)}(2)$  by  $\text{N}_2\text{O}$  or pyridine oxide which results in the generation of  $\text{NacNacGa}(\text{O})$  as a monomeric oxide intermediate leading to the C–H bond activation (Scheme 32).<sup>54</sup> The oxidation of  $^{\text{Dipp}}\text{NacNacGa(i)}(2)$  by using pyridine oxide led to the C–H bond activation of pyridine oxide, yielding  $^{\text{Dipp}}\text{NacNacGa}(\text{OH})(\eta^1(\text{C}), \kappa^1(\text{O})\text{-}o\text{-C}_5\text{H}_4\text{N-O})$  (**142**), and pyridine. A similar reaction between  $^{\text{Dipp}}\text{NacNacGa(i)}(2)$  and  $\text{N}_2\text{O}$  in the presence of pyridine and cyclohexanone leads to  $^{\text{Dipp}}\text{NacNacGa}(\text{OH})(o\text{-C}_5\text{H}_4\text{N})$  (**143**) and  $^{\text{Dipp}}\text{NacNacGa}(\text{OH})(\text{OC}_6\text{H}_9)$  (**144**), respectively. The oxidation of  $^{\text{Dipp}}\text{NacNacGa(i)}(2)$  in the presence of  $\text{Ph}_2\text{C=O}$  resulted in the isolation of compound  $^{\text{Dipp}}\text{NacNacGa}(\kappa^2\text{-O}_2\text{CPh}_2)$  (**145**), formed from the sequential oxidation and cyclization. The *in situ* oxidation of the mixtures of  $^{\text{Dipp}}\text{NacNacGa(i)}(2)$  with  $\text{O=SMe}_2$  and  $\text{O=PEt}_3$  resulted in the  $\text{sp}^3$  C–H bond cleavage yielding compounds  $^{\text{Dipp}}\text{NacNacGa}$



Scheme 32 Sequential oxidation/C–H activation of Ga(i).

$(\text{CH}_2\text{S(=O)Me})\text{OH}$  (**146**) and  $^{\text{Dipp}}\text{NacNacGa}(\text{CH}(\text{Me})\text{P(=O)Et}_2)\text{OH}$  (**147**), respectively.

### 3. Conclusions and perspectives

In conclusion, we report monomeric aluminum and gallium carbenoid complexes supported by  $\beta$ -diketiminate ligands which possess a lone pair of electrons and a formally vacant p orbital. These features afford high electrophilic and nucleophilic reactivity that could be used in bond activation and cleavage upon reactions with small molecules. The aluminum and gallium carbenoid complexes undergo a series of oxidative addition reactions with  $\sigma$  H–X and E'–E bonds where E is an element from groups 13 to 16. These compounds also demonstrate the oxidative cleavage of multiple bonds and enthalpically strong bonds ( $\text{M-X}$ ,  $\text{E'=E}$ ). An extension of the synthetic approach is presented in this review for the synthesis of Group 13 metalloid complexes that consist of an unsupported M'–M ( $\text{M}' = \text{Al}, \text{Ga}$ ) bond. The oxidative cleavage of multiple bonds shows new and unusual reactivities. These reactivities have opened up a new realm in aluminum and gallium chemistry that could lead to many new products. Nevertheless, the compounds with low valent aluminum and gallium are still showing some limitations in catalytic applications.

However, dialumene (**I**) promoted both the catalytic and stoichiometric reduction of  $\text{CO}_2$  to value added C1 products, which is the first example of catalysis using a homonuclear main-group multiple bond. It is important to explore reductive elimination of C–C bonds, which leads to reversible bond activation paving the way towards catalytic applications. Recent developments in the isolation of aluminyl complexes (**II**) will likely extend the low oxidation state Al chemistry that is used to activate the C–C bonds. We look forward to conducting

Scheme 31 Oxidative addition of  $\sigma$  bonds to Al(i) and Ga(i) compounds, respectively.



further studies of the Al(i) and Ga(i) complexes which will result in more unprecedented bond cleavage reactions and important future applications in catalysis.

## Conflicts of interest

There are no conflicts to declare.

## Acknowledgements

H. W. R. thanks the DFG for support of this work (RO 224/71-1). We also thank Prof. Z. Yang from the Beijing Institute of Technology for helpful discussions. This work is dedicated to Professor Reinhold Tacke on the occasion of his 70th birthday.

## Notes and references

- (a) R. H. Holm, *Chem. Rev.*, 1987, **87**, 1401–1449; (b) N. Miyaoura and A. Suzuki, *Chem. Rev.*, 1995, **95**, 2457–2483; (c) E. M. McGarrigle and D. G. Gilheany, *Chem. Rev.*, 2005, **105**, 1563–1602; (d) I. A. I. Mkhalid, J. H. Barnard, T. B. Marder, J. M. Murphy and J. F. Hartwig, *Chem. Rev.*, 2010, **110**, 890–931; (e) B. Sarkar, D. Schweinfurth, N. Deibel and F. Weisser, *Coord. Chem. Rev.*, 2015, **293–294**, 250–262.
- (a) C. Dohmeier, C. Robl, M. Tacke and H. Schnöckel, *Angew. Chem., Int. Ed. Engl.*, 1991, **30**, 564–565, (*Angew. Chem.*, 1991, **103**, 594–595); (b) S. Schulz, H. W. Roesky, H.-J. Koch, G. M. Sheldrick, D. Stalke and A. Kuhn, *Angew. Chem., Int. Ed. Engl.*, 1993, **32**, 1729–1731.
- (a) W. Uhl, *Angew. Chem., Int. Ed. Engl.*, 1993, **32**, 1386–1397, (*Angew. Chem.*, 1993, **105**, 1449–1461); (b) C. Dohmeier, D. Loos and H. Schnöckel, *Angew. Chem., Int. Ed. Engl.*, 1996, **35**, 129–149, (*Angew. Chem.*, 1996, **108**, 141–161).
- A. H. Cowley, *Chem. Commun.*, 2004, 2369–2375.
- (a) L. Bourget-Merle, M. F. Lappert and J. R. Severn, *Chem. Rev.*, 2002, **102**, 3031–3066; (b) Y. Tsai, *Coord. Chem. Rev.*, 2012, **256**, 722–758; (c) C. Chen, S. M. Bellows and P. L. Holland, *Dalton Trans.*, 2015, **44**, 16654–16670.
- (a) H. W. Roesky and S. S. Kumar, *Chem. Commun.*, 2005, 4027–4038; (b) S. Nagendran and H. W. Roesky, *Organometallics*, 2008, **27**, 457–492; (c) M. Asay, C. Jones and M. Driess, *Chem. Rev.*, 2011, **111**, 354–396; (d) W. Li, X. Ma, M. G. Walawalkar, Z. Yang and H. W. Roesky, *Coord. Chem. Rev.*, 2017, **350**, 14–29; (e) Y. Liu, J. Li, X. Ma, Z. Yang and H. W. Roesky, *Coord. Chem. Rev.*, 2018, **374**, 387–415; (f) T. Chu and G. I. Nikonov, *Chem. Rev.*, 2018, **118**, 3608–3680; (g) V. Nesterov, D. Reiter, P. Bag, P. Frisch, R. Holzner, A. Porzelt and S. Inoue, *Chem. Rev.*, 2018, **118**, 9678–9872; (h) P. Bag, C. Weetman and S. Inoue, *Angew. Chem., Int. Ed.*, 2018, **57**, 14394–14413.
- (a) P. P. Power, *Nature*, 2010, **463**, 171–177; (b) C. Weetman and S. Inoue, *ChemCatChem*, 2018, **10**, 4213–4228; (c) R. L. Melen, *Science*, 2019, **363**, 479–484.
- (a) C. Cui, H. W. Roesky, H.-G. Schmidt, M. Noltemeyer, H. Hao and F. Cimpoesu, *Angew. Chem., Int. Ed.*, 2000, **39**, 4274–4276; (b) X. Li, X. Cheng, H. Song and C. Cui, *Organometallics*, 2007, **26**, 1039–1043; (c) H. Zhu, R. B. Oswald, H. Fan, H. W. Roesky, Q. Ma, Z. Yang, H.-G. Schmidt, M. Noltemeyer, K. Starke and N. S. Hosmane, *J. Am. Chem. Soc.*, 2006, **128**, 5100–5108.
- Y. García-Rodeja, F. M. Bickelhaupt and I. Fernández, *Chem. – Eur. J.*, 2016, **22**, 13669–13676.
- (a) P. Bag, A. Porzelt, P. J. Altmann and S. Inoue, *J. Am. Chem. Soc.*, 2017, **139**, 14384–14387; (b) C. Weetman, P. Bag, T. Szilvási, C. Jandl and S. Inoue, *Angew. Chem., Int. Ed.*, 2019, **58**, 10961–10965.
- (a) J. Hicks, P. Vasko, J. M. Goicoechea and S. Aldridge, *Nature*, 2018, **557**, 92–95; (b) J. Hicks, A. Mansikkamäki, P. Vasko, J. M. Goicoechea and S. Aldridge, *Nat. Chem.*, 2019, **11**, 237–241; (c) J. Hicks, P. Vasko, J. M. Goicoechea and S. Aldridge, *J. Am. Chem. Soc.*, 2019, **141**, 11000–11003.
- (a) R. J. Schwamm, M. D. Anker, M. Lein and M. P. Coles, *Angew. Chem., Int. Ed.*, 2019, **58**, 1489–1493; (b) M. D. Anker and M. P. Coles, *Angew. Chem., Int. Ed.*, 2019, **58**, 13452–13455.
- (a) J. Hicks, A. Heilmann, P. Vasko, J. M. Goicoechea and S. M. Aldridge, *Angew. Chem., Int. Ed.*, 2019, **58**, 17265–17268; (b) D. Anker and M. P. Coles, *Angew. Chem., Int. Ed.*, 2019, **58**, 18429–18433.
- (a) A. Hofmann, C. Pranckevicius, T. Tröster and H. Braunschweig, *Angew. Chem., Int. Ed.*, 2019, **58**, 3625–3628; (b) S. K. Møllerup, Y. Cui, F. Fantuzzi, P. Schmid, J. T. Goettel, G. Bélanger-Chabot, M. Arrowsmith, M. Krummenacher, Q. Ye, V. Engel, V. Engels and H. Braunschweig, *J. Am. Chem. Soc.*, 2019, **141**, 16954–16960; (c) S. Kurumada, S. Takamori and M. Yamashita, *Nat. Chem.*, 2020, **12**, 36–39.
- (a) S. L. Choong, W. D. Woodul, A. Stasch, C. Schenk and C. Jones, *Aust. J. Chem.*, 2011, **64**, 1173–1176; (b) C. P. Sindlinger, S. R. Lawrence, S. Acharya, C. A. Ohlin and A. Stasch, *Dalton Trans.*, 2017, **46**, 16872–16877; (c) A. L. Hawley, C. A. Ohlin, L. Fohlmeister and A. Stasch, *Chem. – Eur. J.*, 2017, **23**, 447–455.
- (a) E. S. Schmidt, A. Jockisch and H. Schmidbaur, *J. Am. Chem. Soc.*, 1999, **121**, 9758–9759; (b) E. S. Schmidt, A. Schier and H. Schmidbaur, *J. Chem. Soc., Dalton Trans.*, 2001, 505–507; (c) R. J. Baker, R. D. Farley, C. Jones, M. Kloth and D. M. Murphy, *J. Chem. Soc., Dalton Trans.*, 2002, 3844–3850; (d) I. L. Fedushkin, A. N. Lukoyanov, G. K. Fukin, S. Y. Ketkov, M. Hummert and H. Schumann, *Chem. – Eur. J.*, 2008, **14**, 8465–8468; (e) I. L. Fedushkin, A. N. Lukoyanov, A. N. Tishkina, G. K. Fukin, K. A. Lyssenko and M. Hummert, *Chem. – Eur. J.*, 2010, **16**, 7563–7571; (f) I. L. Fedushkin, A. N. Lukoyanov, G. K. Fukin, S. Y. Ketkov, M. Hummert and H. Schumann, *Chem. – Eur. J.*, 2008, **14**, 8465–8468; (g) I. L. Fedushkin, A. N. Lukoyanov, A. N. Tishkina, G. K. Fukin,



- K. A. Lyssenko and M. Hummert, *Chem. – Eur. J.*, 2010, **16**, 7563–7571; (h) D. Dange, S. L. Choong, C. Schenk, A. Stasch and C. Jones, *Dalton Trans.*, 2012, **41**, 9304–9315; (i) C. Jones, P. C. Junk, J. A. Platts and A. Stasch, *J. Am. Chem. Soc.*, 2006, **128**, 2206–2207; (j) G. Jin, C. Jones, P. C. Junk, A. Stasch and W. D. Woodul, *New J. Chem.*, 2008, **32**, 835–842; (k) J. Overgaard, C. Jones, D. Dange and J. A. Platts, *Inorg. Chem.*, 2011, **50**, 8418–8426; (l) M. C. Kuchta, J. B. Bonanno and G. Parkin, *J. Am. Chem. Soc.*, 1996, **118**, 10914–10915; (m) R. J. Wright, M. Brynda, J. C. Fetting, A. R. Betzer and P. P. Power, *J. Am. Chem. Soc.*, 2006, **128**, 12498–12509.
- 17 N. Saito, J. Takaya and N. Iwasawa, *Angew. Chem., Int. Ed.*, 2019, **58**, 9998–10002.
- 18 (a) C. Jones, *Nat. Rev. Chem.*, 2017, **1**, 59; (b) S. F. McWilliams and P. L. Holland, *Acc. Chem. Res.*, 2015, **48**, 2059–2065.
- 19 P. J. Chirik, *Inorg. Chem.*, 2011, **50**, 9737–9740.
- 20 N. J. Hardman, B. E. Eichler and P. P. Power, *Chem. Commun.*, 2000, 1991–1992.
- 21 J. A. B. Abdalla, I. M. Riddlestone, R. Tirfoin and S. Aldridge, *Angew. Chem., Int. Ed.*, 2015, **54**, 5098–5102.
- 22 R. Y. Kong and M. R. Crimmin, *J. Am. Chem. Soc.*, 2018, **140**, 13614–13617.
- 23 R. Y. Kong and M. R. Crimmin, *Chem. Commun.*, 2019, **55**, 6181–6184.
- 24 (a) C. Bakewell, A. J. P. White and M. R. Crimmin, *Angew. Chem., Int. Ed.*, 2018, **57**, 6638–6642; (b) C. Bakewell, A. J. P. White and M. R. Crimmin, *Chem. Sci.*, 2019, **10**, 2452–2458.
- 25 A. Paparo, C. D. Smith and C. Jones, *Angew. Chem., Int. Ed.*, 2019, **58**, 11459–11463.
- 26 B. Li, S. Kundu, H. Zhu, H. Keil, R. Herbst-Irmer, D. Stalke, G. Frenking, D. M. Andradac and H. W. Roesky, *Chem. Commun.*, 2017, **53**, 2543–2546.
- 27 S. Sinhababu, S. Kundu, A. N. Paesch, R. Herbst-Irmer, D. Stalke and H. W. Roesky, *Eur. J. Inorg. Chem.*, 2018, 2237–2240.
- 28 (a) S. Brand, H. Elsen, J. Langer, W. A. Donaubauer, F. Hampel and S. Harder, *Angew. Chem., Int. Ed.*, 2018, **57**, 14169–14173; (b) T. N. Hooper, M. Garçon, A. J. P. White and M. R. Crimmin, *Chem. Sci.*, 2018, **9**, 5435–5440; (c) S. Brand, H. Elsen, J. Langer, S. Grams and S. Harder, *Angew. Chem., Int. Ed.*, 2019, **58**, 15496–15503.
- 29 C. Ganesamoorthy, D. Bläser, C. Wölper and S. Schulz, *Angew. Chem., Int. Ed.*, 2014, **53**, 11587–11591.
- 30 G. Prabusankar, C. Gemel, P. Parameswaran, C. Flener, G. Frenking and R. A. Fischer, *Angew. Chem., Int. Ed.*, 2009, **48**, 5526–5529.
- 31 C. Ganesamoorthy, D. Bläser, C. Wölper and S. Schulz, *Chem. Commun.*, 2014, **50**, 12382–12384.
- 32 G. Prabusankar, C. Gemel, M. Winter, R. W. Seidel and R. A. Fischer, *Chem. – Eur. J.*, 2010, **16**, 6041–6047.
- 33 G. Prabusankar, S. Gonzalez-Gallardo, A. Doddi, C. Gemel, M. Winter and R. A. Fischer, *Eur. J. Inorg. Chem.*, 2010, **28**, 4415–4418.
- 34 C. Ganesamoorthy, G. Bendt, D. Bläser, C. Wölper and S. Schulz, *Dalton Trans.*, 2015, **44**, 5153–5159.
- 35 C. Ganesamoorthy, D. Bläser, C. Wölper and S. Schulz, *Organometallics*, 2015, **34**, 2991–2996.
- 36 C. Ganesamoorthy, C. Helling, C. Wölper, W. Frank, E. Bill, G. E. Cutsail III and S. Schulz, *Nat. Commun.*, 2018, **9**, 87–93.
- 37 C. Helling, C. Wölper and S. Schulz, *J. Am. Chem. Soc.*, 2018, **140**, 5053–5056.
- 38 (a) L. Tuscher, C. Ganesamoorthy, D. Bläser, C. Wölper and S. Schulz, *Angew. Chem., Int. Ed.*, 2015, **54**, 10657–10661; (b) L. Tuscher, C. Helling, C. Ganesamoorthy, J. Kreger, C. Wölper, W. Frank, A. S. Nizovtsev and S. Schulz, *Chem. – Eur. J.*, 2017, **23**, 12297–12304.
- 39 J. Kreger, C. Ganesamoorthy, L. John, C. Wölper and S. Schulz, *Chem. – Eur. J.*, 2018, **24**, 9157–9164.
- 40 J. Krüger, C. Wölper, L. John, L. Song, P. R. Schreiner and S. Schulz, *Eur. J. Inorg. Chem.*, 2019, **11–12**, 1669–1678.
- 41 U. Chakraborty, B. Mühldorf, N. J. C. van Velzen, B. de Bruin, S. Harder and R. Wolf, *Inorg. Chem.*, 2016, **55**, 3075–3078.
- 42 (a) L. Tuscher, C. Helling, C. Wölper, W. Frank, A. S. Nizovtsev and S. Schulz, *Chem. – Eur. J.*, 2018, **24**, 3241–3250; (b) L. Song, J. Schoening, C. Wölper, S. Schulz and P. R. Schreiner, *Organometallics*, 2019, **38**, 1640–1647.
- 43 (a) M. R. Crimmin, M. J. Butler and A. J. P. White, *Chem. Commun.*, 2015, **51**, 15994–15996; (b) T. Chu, Y. Boyko, I. Korobkov and G. I. Nikonov, *Organometallics*, 2015, **34**, 5363–5365.
- 44 (a) A. Koner, B. M. Gabidullin, Z. Kelemen, L. Nyulászi, G. I. Nikonov and R. Streubel, *Dalton Trans.*, 2019, **48**, 8248–8253; (b) T. Chu, S. F. Vyboishchikov, B. Gabidullin and G. I. Nikonov, *Angew. Chem., Int. Ed.*, 2016, **55**, 13306–13311.
- 45 T. Chu, Y. Boyko, I. Korobkov, L. G. Kuzmina, J. A. K. Howard and G. I. Nikonov, *Inorg. Chem.*, 2016, **55**, 9099–9104.
- 46 L. Kong, R. Ganguly, Y. Li and R. Kinjo, *Chem. – Eur. J.*, 2016, **22**, 1922–1925.
- 47 T. Chu, S. F. Vyboishchikov, B. M. Gabidullin and G. I. Nikonov, *J. Am. Chem. Soc.*, 2017, **139**, 8804–8807.
- 48 (a) T. Chu, S. F. Vyboishchikov, B. M. Gabidullin and G. I. Nikonov, *Inorg. Chem.*, 2017, **56**, 5993–5997; (b) A. Dmitrienko, J. F. Britten, D. Spasyuk and G. I. Nikonov, *Chem. – Eur. J.*, 2020, **26**, 206–211.
- 49 L. L. Liu, J. Zhou, L. L. Cao and D. W. Stephan, *J. Am. Chem. Soc.*, 2019, **141**, 16971–16982.
- 50 A. Kassymbek, J. F. Britten, D. Spasyuk, B. Gabidullin and G. I. Nikonov, *Inorg. Chem.*, 2019, **58**, 8665–8672.
- 51 T. Chu, I. Korobkov and G. I. Nikonov, *J. Am. Chem. Soc.*, 2014, **136**, 9195–9202.
- 52 A. Seifert, D. Scheid, G. Linti and T. Zessin, *Chem. – Eur. J.*, 2009, **15**, 12114–12120.
- 53 E. Herappe-Mejía, K. Trujillo-Hernández, J. C. Garduño-Jiménez, F. Cortés-Guzmán, D. Martínez-Otero and V. Jancik, *Dalton Trans.*, 2015, **44**, 16894–16902.
- 54 A. Kassymbek, S. F. Vyboishchikov, B. M. Gabidullin, D. Spasyuk, M. Pilkington and G. I. Nikonov, *Angew. Chem., Int. Ed.*, 2019, **58**, 18102–18107.

